

Transverse Electrical Resistivity Evaluation of Rod Unidirectional Carbon Fiber-Reinforced Composite Using Eddy Current Method

O. A. Safer¹, S. Bensaid², D. Trichet³, and G. Wasselynck³

¹Laboratoire de Génie Electrique, University de M'sila, M'sila 28000, Algeria

²Laboratoire des Matériaux et du Développement Durable, Université de Bouira, Bouira 10000, Algeria

³Institut de Recherche en Energie Electrique de Nantes Atlantique, 44600 Saint-Nazaire, France

This paper proposes a simple approach to evaluate a transverse electrical resistivity of a rod unidirectional carbon fiber-reinforced composites (UD-CFRCs). The method is based on eddy current technique. The model is associated with inverse problem method that consists of minimizing the difference between the computed and measured resistances. The ant colony algorithm which is a kind of heuristic minimizing algorithm based on population exploration is used to get transverse electrical resistivity. The findings of the work are summarized as the following. First, it was demonstrated that the induced power in the UD-CFRC and the resistance of the coil are independent of the value of longitudinal resistivity. Then, the electrical resistance is computed using direct problem which is formulated with the 2-D axisymmetric finite-element method. After that, the identified resistivity, which obtained with the inverse problem, is introduced in the direct problem to compute resistance. Finally, the confrontation between the computed resistance and the measured one shows a significant concordance between the two.

Index Terms—Composite materials, conductivity measurement, eddy currents, finite-element analysis, inverse problem.

I. INTRODUCTION

DUE to their high performances, carbon fiber-reinforced composite (CFRC) rods have large applications in the manufacturing industries such as aerospace industry and civil building. They are mainly used to manufacture bridges and cable structures of tower constructions [1]. A composite can be broadly defined as an arrangement of two or more materials that retain their macrostructure resulting in a material that can be designed to have improved properties than the constituents alone. The rods, which consist of carbon fibers plies backed with a diameter close to a few micrometers, are glued together in epoxy filled matrix in order to build cylindrical shape [2].

The defects related to rod CFRC that appear during unidirectional CFRC (UD-CFRC) rod manufacture such as fiber break and bonding lack, affect directly the construction strength [3], [4]. Yet, delamination which is due to the fatigue is the most usual defect in rod CFRC. To detect these defects, non-destructive eddy current method can be used [4], [5]. To better apply this technique, it is necessary to evaluate the electrical resistivity in each direction of the rod [6].

The longitudinal electrical resistivity can be measured by using a volt-ampere-metric method. However, due to the fiber insulated in thermoplastic, the important number of fiber in 1 mm^2 and the contact issues between fibers, it is not easy to evaluate the transverse resistivity using the afore mentioned method.

UD-CFRC rod has a strong anisotropy due to the unique orientation of the fibers. However, the important number of carbon fibers impregnated in the rod and their size compared to global dimensions make difficult to take them into account in the model [6], [7]. The microscopic electrical resistivity of the composite materials is then replaced by a

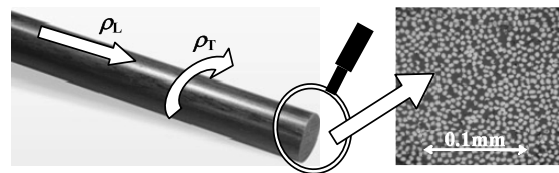


Fig. 1. UD-CFRC rod and the microscopic picture.

homogenized anisotropic tensor [8] with the principal the longitudinal resistivity (ρ_L) and the transverse resistivity (ρ_T) components (Fig. 1). The electrical anisotropy depends on the volume fraction of and the fiber orientation in the composite material; hence, ρ_L varies between 2×10^{-5} and $10^{-3} \Omega \cdot \text{m}$, while ρ_T between 5×10^{-3} and $10^{-1} \Omega \cdot \text{m}$ [8], [9].

In this paper, a simple approach is proposed to evaluate the homogenized transverse resistivity of UD-CRFC rod, using contactless method based on eddy currents which are induced by a multi-layered solenoid coil.

In this context, the Cedrat/Flux 3-D software is used to compute the value of induced power and to study the direction of induced currents in the UD-CFRC rod according to the longitudinal resistivity. This paper allowed to justify the use of the 2-D model and to free ourselves from the difficulties of using the 3-D model. A 2-D problem can be easily formulated using magnetic potential vector and solved with finite-element method (FEM) implemented in MATLAB. The inverse problem goal function is minimized using the ant colony algorithm (ACA) in order to evaluate the transverse electrical conductivity according to measurement of the variation of resistivity of the coil [6], [7]. The measures are performed using a precision LCR meter.

II. PROBLEM MODELING

A. 2-D Model Justifying

To justify the use of the 2-D model one realizes the study of eddy currents 3-D behavior according to the longitudinal

Manuscript received June 27, 2017; revised August 30, 2017; accepted September 6, 2017. Date of publication October 2, 2017; date of current version February 21, 2018. Corresponding author: S. Bensaid (e-mail: s.bensaid@univ-bouira.dz).

Digital Object Identifier 10.1109/TMAG.2017.2751962

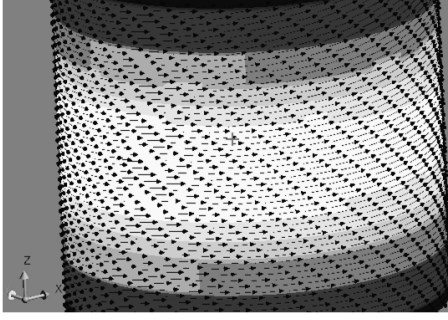


Fig. 2. 3-D eddy current direction in the CFRC rod for frequency = 2 MHz ($\rho_T = \rho_l = \rho_x = \rho_y = \rho_z = 0.013 \Omega \cdot m$).

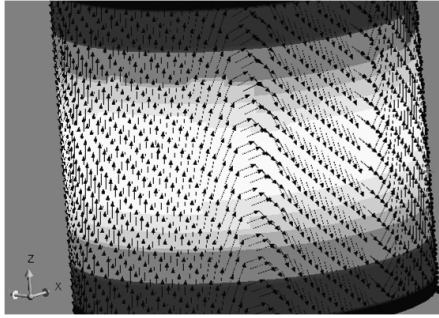


Fig. 3. 3-D eddy current direction in the CFRC rod for frequency = 2 MHz ($\rho_L = \rho_z = 10^{-5} \Omega \cdot m$, $\rho_T = \rho_x = \rho_y = 0.013 \Omega \cdot m$).

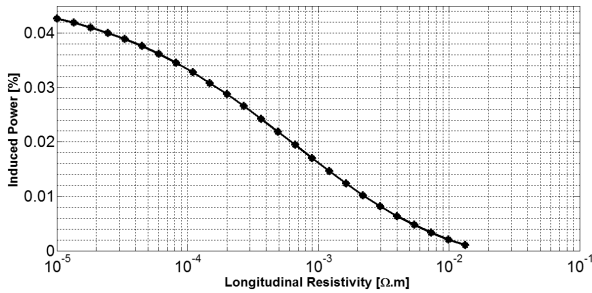


Fig. 4. Total induced in the CFRC rod for frequency = 2 MHz as a function of rod longitudinal resistivity.

resistivity of the UD-CFRC. The Cedrat/Flux 3-D software is used.

At the 2 MHz frequency and for no change value of transverse resistivity $\rho_T = \rho_x = \rho_y = 0.013 \Omega \cdot m$, the study shows that the eddy currents have the same components as the source currents for the isotropic tensor of electrical resistivity $\rho_L = \rho_T$ (Fig. 2).

The longitudinal induced current component appears at the low value of the longitudinal electrical resistivity (Fig. 3).

On the other hand, there are a variation lower than 0.04% of induced power (Fig. 4) and resistance of a solenoid coil (Fig. 5), according to the variation of longitudinal electrical resistivity from 10^{-5} to $0.7 \times 10^{-2} \Omega \cdot m$.

Therefore, the longitudinal component of induced currents has no influence on the total induced power or the resistance of the solenoid coil. Thus, the influential induced currents are

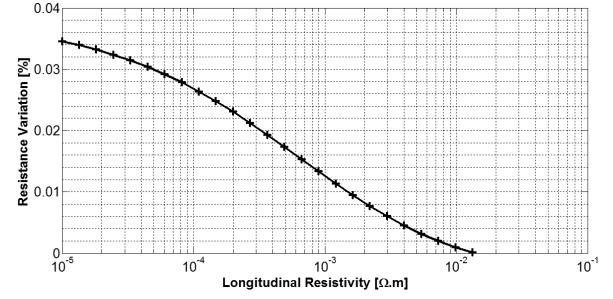


Fig. 5. Resistance variation of solenoid coil frequency = 2 MHz as a function of rod longitudinal resistivity.

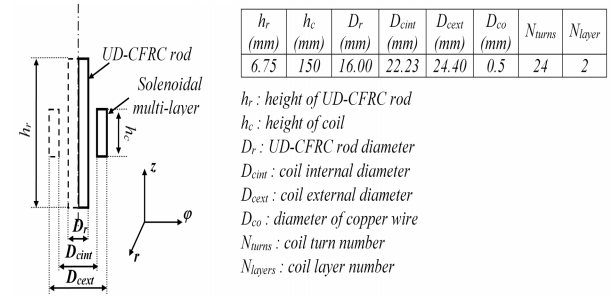


Fig. 6. Axisymmetric geometric model.

all in the transverse direction (xy) which is the path of the source currents. Hence, the 2-D model can be used to compute resistance of the solenoid coil. Moreover, the electrical conductivity is not affected by thermal phenomena due to the low induced power in CFRC.

B. 2-D Axisymmetric Model

The numerical model can be expressed in 2-D axisymmetric domain using $\vec{A} - V$ formulation, named, potentials successively, magnetic vector and electrical scalar. Fig. 6 shows the geometric model and characteristic dimensions.

To compute the resistance of coil which is due to the induced current reaction of the UD-CFRC rod, the following electromagnetic equation must be solved under the geometric domain (Fig. 6):

$$-\iint_{\Omega} \frac{\partial}{\partial r} \left(\frac{1}{r \mu_0} \frac{\partial A'}{\partial r} \right) - \frac{\partial}{\partial z} \left(\frac{1}{r \mu_0} \frac{\partial A'}{\partial z} \right) + j \frac{\omega}{r \rho_t} A' = J_{s\phi} \quad (1)$$

where $A'(0, r A_{\phi}, 0)$ (T · m²) is the modified magnetic vector potential, ρ_t (Ω · m) is the transverse electrical resistivity of the UD-CFRC rod, ω is the electrical pulsation (rad/s), μ_0 is the magnetic permeability of air, and $J_{s\phi}(0, J_{s\phi}, 0)$ (A/m²) is the source current density. ρ_t is the transverse resistivity that depending the skin thickness effect δ who is given by

$$\delta = \sqrt{\frac{2}{\omega \rho_t \mu_0}} \quad (2)$$

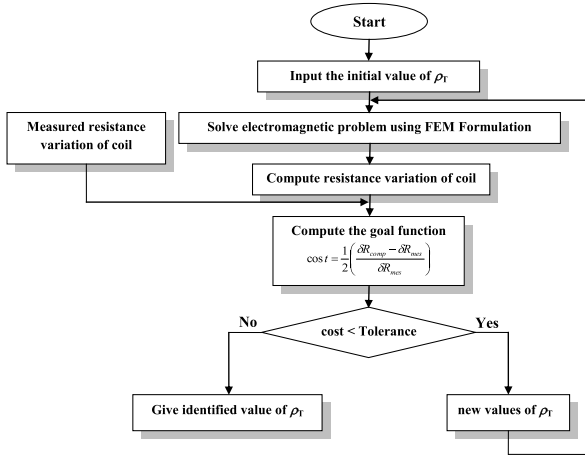


Fig. 7. Inverse problem algorithm.

The FEM formulation can be expressed as

$$\begin{aligned}
 & - \sum_{j=1}^N \left(\iint_{\Omega} \frac{1}{\mu_0 r} \vec{\nabla} \alpha_i \vec{\nabla} \alpha_j dr dz \right) A_j \\
 & + j\omega \sum_{j=1}^N \left(\iint_{\Omega} \alpha_i \alpha_j \frac{1}{r \rho_T} dr dz \right) A_j \\
 & = \iint_{\Omega} \alpha_i J_{s\phi} dr dz
 \end{aligned} \quad (3)$$

where N is the node number and α_i and α_j are the finite-element interpolation functions. The modified magnetic vector potential A' is computed in all regions (rod, air, coil). The coil resistance variation δR_{comp} is computed using the following expression:

$$\delta R_{\text{comp}} = -2 \cdot \pi \cdot \omega \cdot N_{\text{turns}}^2 \cdot \text{imag}(\text{mean}(A')) \quad (4)$$

where N_{turns} is the number of turns and imag is the imaginary part.

C. Inverse Problem Applied to Resistivity Identification

The resistance of the probe is measured using a precision LCRmeter. The resistance variation of the coil is calculated using a 2-D axisymmetric FEM model and then compared with that measured until the convergence criterion of the objective function as illustrated in (5). The transverse resistivity then is identified. These steps are illustrated by the inverse problem algorithm (Fig. 7).

The inverse problem goal function is written as

$$\text{cost} = \frac{1}{2} \left(\frac{\delta R_{\text{comp}} - \delta R_{\text{mes}}}{\delta R_{\text{mes}}} \right) \quad (5)$$

where δR_{mes} and δR_{comp} , respectively, is the measured and the computed coil resistance variation with and without the presence of UD-CFRC rod.

ACA is applied to minimize the inverse problem goal function in order to get the transverse electrical resistivity.

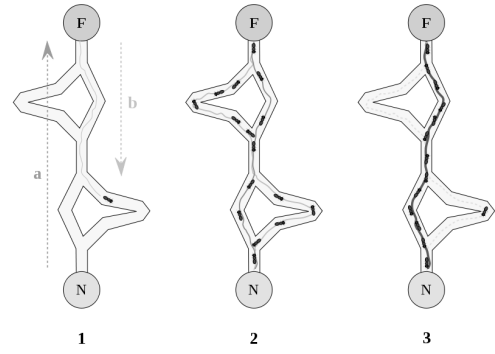


Fig. 8. ACA steps.

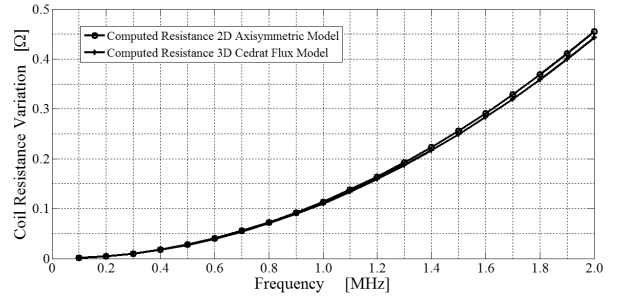


Fig. 9. 2-D and 3-D computed resistance variations of the solenoid coil as a function of frequency.

This algorithm is a probabilistic technique for solving computational problems which can be reduced to find good paths through graphs.

As shown in Fig. 8, the steps of the ACA [10]–[12] are the following.

- 1) The first ant finds the food source (F) via any path (a), then returns to the nest (N) leaving behind a pheromone trail (b).
- 2) The ants use the four paths indifferently, but the reinforcement of the track makes the shortest route more attractive.
- 3) The ants take the shortest route; the long portions of the other paths lose their pheromone trail.

III. RESULTS AND DISCUSSION

A. 2-D Axisymmetric Model Validation

In order to check the use of 2-D axisymmetric model, resistance variation of the solenoid coil is computed under 3-D and 2-D model.

Fig. 9 shows the comparison between the 2-D and 3-D computed resistance variations as a function of frequency from 0.1 to 2 MHz and for the case of resistivity tensor components given by $\rho_L = 10^{-5} \Omega \cdot \text{m}$ and $\rho_T = 0.013 \Omega \cdot \text{m}$. The maximum error observed is less than 1%.

Fig. 10 shows the comparison between the 2-D and 3-D computed resistance variations of the solenoid coil as a function of transverse resistivity ρ_T in the range of 0.02–0.1 $\Omega \cdot \text{m}$ at frequency equal to 2 MHz and longitudinal resistivity ρ_L fixed at 50 $\mu\Omega \cdot \text{m}$. The maximum error is less than 2%.

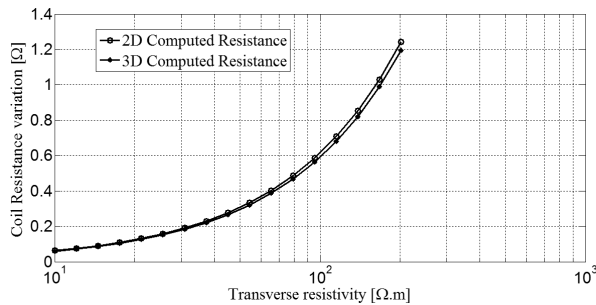


Fig. 10. 2-D and 3-D computed resistance variations of the solenoid coil as a function of transverse resistivity ($0.02\text{--}0.1 \Omega \cdot \text{m}$) at frequency equal to 2 MHz and $\rho_L = 50 \mu\Omega \cdot \text{m}$.

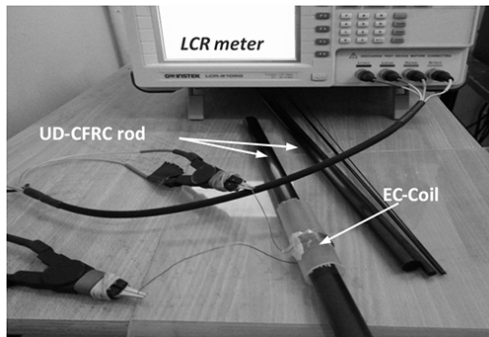


Fig. 11. Experimental setup.

These results allow us to confirm the validity of using of the 2-D axisymmetric model.

B. Resistivity Evaluation and Validation

To identify the transverse resistivity, we use an experimental setup (Fig. 11) performed with a precision LRCmeter, UD-CFRC rod, and copper wires. The dimensions of rod and multi-layers solenoid coil are given in Fig. 6.

The longitudinal resistivity of the UD-CFRC rod is measured using the two-point method which is $\rho_L = 50 \mu\Omega \cdot \text{m}$.

The obtained transverse resistivity value, using inverse problem method at 2 MHz frequency, is $0.01316 \Omega \cdot \text{m}$.

This value of resistivity is introduced in the 2-D axisymmetric model to compute the coil resistance variation for frequency range of 0.1–2 MHz. The resistance of coil is measured using a precision LCR meter (Fig. 11).

Fig. 12 shows the comparison between the 2-D computed resistance variation of the coil and the measured one.

The maximum error between the two results is less than 2%.

IV. CONCLUSION

In this paper, eddy current non-destructive evaluation technique in association with inverse problem method is used to evaluate the transverse electrical resistivity of the UD-CFRC rod. A 3-D Cedrat/Flux simulation shows clearly that the longitudinal electrical resistivity has no influence to the path of the influential eddy currents created in the UD-CFRC rod and their value. Therefore, the resistance can be computed using a 2-D axisymmetric model. Inverse problem is applied to identify the transverse electrical resistivity. ACA is used to

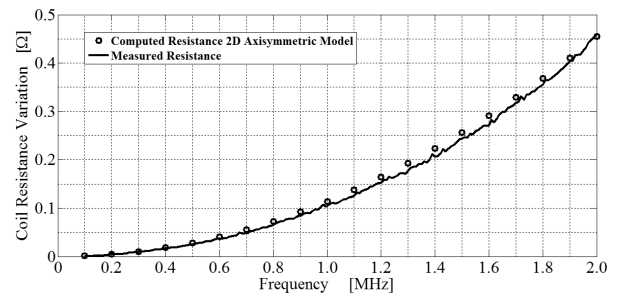


Fig. 12. 2-D computed resistance variation of the solenoid coil and the measured one as a function of frequency for identified resistivity of the UD-CFRC rod.

minimize goal function of the inverse problem. The identified resistivity is introduced in the direct model (2-D axisymmetric model) to compute resistance. The confrontation between the computed resistance and the measured one shows a very good concordance.

In order to generalize the results of this paper, the study must be carried out on UD-CFRC with planar structures.

ACKNOWLEDGMENT

The authors would like to thank H. Bensaid English Teacher at Tizi-Ouzou University and M. Amara for their advices and help.

REFERENCES

- [1] Y. Liu, B. Zwingmann, and M. Schlaich, "Carbon fiber reinforced polymer for cable structures—A review," *Polymers*, vol. 7, no. 10, pp. 2078–2099, 2015.
- [2] C. A. Burningham, C. P. Pantelides, and L. D. Reaveley, "Repair of reinforced concrete deep beams using post-tensioned CFRP rods," *Compos. Struct.*, vol. 125, pp. 256–265, Jul. 2015.
- [3] L. V. da Silva, F. W. da Silva, J. R. Tarpani, M. M. de C. Forte, and S. C. Amico, "Ageing effect on the tensile behavior of pultruded CFRP rods," *Mater. Des.*, vol. 110, pp. 245–254, Nov. 2016.
- [4] K.-N. Antin, T. P. Santos, and P. Vilaça, "Detection of damage in unidirectional carbon fiber composite rods using eddy current probes," in *Proc. Sampe Eur. Conf.*, Amiens, France, Sep. 2015, pp. 15–17.
- [5] R. Kažys, R. Raišutis, E. Žukauskas, L. Mažeika, and A. Vladišauskas, "Air-coupled ultrasonic testing of CFRP rods by means of guided waves," *Phys. Proc.*, vol. 3, no. 1, pp. 185–192, 2010.
- [6] S. Bensaid, D. Trichet, and J. Fouladgar, "Electrical conductivity identification of composite materials using a 3-D anisotropic shell element model," *IEEE Trans. Magn.*, vol. 45, no. 3, pp. 1859–1862, Mar. 2009.
- [7] S. Bensaid, D. Trichet, and J. Fouladgar, "Optimal design of a rotating eddy-current probe—Application to characterization of anisotropic conductive materials," *IEEE Trans. Magn.*, vol. 51, no. 3, Mar. 2015, Art. no. 6200504.
- [8] G. Wasselynck, D. Trichet, B. Ramdane, and J. Fouladgar, "Microscopic and macroscopic electromagnetic and thermal modeling of carbon fiber reinforced polymer composites," *IEEE Trans. Magn.*, vol. 47, no. 5, pp. 1114–1117, May 2011.
- [9] M. Cacciola, S. Calcagno, G. Megali, D. Pellicano, M. Versaci, and F. C. Morabito, "Eddy current modeling in composite materials," *PIERS Online*, vol. 5, no. 6, pp. 591–595, 2009.
- [10] M. Dorigo and L. M. Gambardella, "Ant colony system: A cooperative learning approach to the traveling salesman problem," *IEEE Trans. Evol. Comput.*, vol. 1, no. 1, pp. 53–66, Apr. 1997.
- [11] L. S. Batista, F. Campelo, F. G. Guimarães, J. A. Ramírez, M. Li, and D. A. Lowther, "Ant colony optimization for the topological design of interior permanent magnet (IPM) machines," *Int. J. Comput. Math. Electr. Electron. Eng.*, vol. 33, no. 3, pp. 927–940, 2014.
- [12] L. C. Echevarría *et al.*, "The fault diagnosis inverse problem with ant colony optimization and ant colony optimization with dispersion," *Appl. Math. Comput.*, vol. 227, pp. 687–700, Jan. 2014.